AIP | Journal of Applied Physics

The influence of pressure on the phase stability of nanocomposite Fe89Zr7B4 during heating from energy dispersive x-ray diffraction

A. M. Leary, M. S. Lucas, P. R. Ohodnicki, S. J. Kernion, L. Mauger et al.

Citation: J. Appl. Phys. **113**, 17A317 (2013); doi: 10.1063/1.4795326
View online: http://dx.doi.org/10.1063/1.4795326
View Table of Contents: http://jap.aip.org/resource/1/JAPIAU/v113/i17
Published by the AIP Publishing LLC.

Report Documentation Page

Form Approved
OMB No. 0704-0188

1. REPORT DATE	2. REPORT TYPE	3. DATES COVERED
MAR 2013		**00-00-2013 to 00-00-2013**

4. TITLE AND SUBTITLE	5a. CONTRACT NUMBER
The influence of pressure on the phase stability of nanocomposite Fe89Zr7B4 during heating from energy dispersive x-ray diffraction	5b. GRANT NUMBER
	5c. PROGRAM ELEMENT NUMBER
6. AUTHOR(S)	5d. PROJECT NUMBER
	5e. TASK NUMBER
	5f. WORK UNIT NUMBER
7. PERFORMING ORGANIZATION NAME(S) AND ADDRESS(ES) **California Institute of Technology,W. M. Keck Laboratory 138-78,Pasadena,CA,91125**	8. PERFORMING ORGANIZATION REPORT NUMBER
9. SPONSORING/MONITORING AGENCY NAME(S) AND ADDRESS(ES)	10. SPONSOR/MONITOR'S ACRONYM(S)
	11. SPONSOR/MONITOR'S REPORT NUMBER(S)

12. DISTRIBUTION/AVAILABILITY STATEMENT
Approved for public release; distribution unlimited

13. SUPPLEMENTARY NOTES

14. ABSTRACT

15. SUBJECT TERMS

16. SECURITY CLASSIFICATION OF:			17. LIMITATION OF ABSTRACT	18. NUMBER OF PAGES	19a. NAME OF RESPONSIBLE PERSON
a. REPORT	b. ABSTRACT	c. THIS PAGE			
unclassified	**unclassified**	**unclassified**	**Same as Report (SAR)**	**4**	

The influence of pressure on the phase stability of nanocomposite $Fe_{89}Zr_7B_4$ during heating from energy dispersive x-ray diffraction

A. M. Leary,[1] M. S. Lucas,[2] P. R. Ohodnicki,[3] S. J. Kernion,[1] L. Mauger,[4] C. Park,[5] C. Kenney-Benson,[5] and M. E. McHenry[1,a)]
[1]*Materials Science and Engineering Department, Carnegie Mellon University, 5000 Forbes Ave; Pittsburgh, Pennsylvania 15213, USA*
[2]*Air Force Research Laboratory, Wright-Patterson AFB, Ohio 45433, USA*
[3]*Division of Chemistry and Surface Science, National Energy Technology Laboratory (NETL), 626 Cochrans Mill Road, Pittsburgh, Pennsylvania 15236, USA*
[4]*California Institute of Technology, W. M. Keck Laboratory 138-78, Pasadena, California 91125, USA*
[5]*High Pressure Collaborative Access Team (HPCAT), Geophysical Laboratory, Carnegie Institution of Washington, 9700 S. Cass Ave., Argonne, Illinois 60439, USA*

(Presented 17 January 2013; received 9 November 2012; accepted 4 December 2012; published online 20 March 2013)

Nanocomposite materials consisting of small crystalline grains embedded within an amorphous matrix show promise for many soft magnetic applications. The influence of pressure is investigated by *in situ* diffraction of hammer milled $Fe_{89}Zr_7B_4$ during heating through the $\alpha \rightarrow \gamma$ Fe transition at 0.5, 2.2, and 4.9 GPa. The changes in primary and secondary crystallization onset are described by diffusion and the energy to form a critical nucleus within the framework of classical nucleation theory. © *2013 American Institute of Physics*. [http://dx.doi.org/10.1063/1.4795326]

Nanocomposite materials consisting of small crystalline grains embedded in an amorphous matrix show promise for soft magnetic applications.[1–3] Of particular research interest is the high frequency switching of nanocomposites for power electronic applications. Thermal,[4] magnetic,[5,6] and strain[7] processing techniques control structure and tailor material performance. Here, we explore pressure effects on crystallization of $Fe_{89}Zr_7B_4$ (NANOPERM[8]) by *in-situ* diffraction with a constant heating rate. Energy dispersive diffraction using a synchrotron source permits high temporal resolution of phase changes under varying temperatures and pressures due to the continuous acquisition of the full diffraction pattern. This affords new insights into the nucleation and growth of crystalline grains from amorphous precursors where the interplay of diffusion and surface energies is not yet fully described.

NANOPERM has demonstrated single phase body-centered-cubic (BCC) α-Fe crystallizing from the as cast amorphous precursor during primary crystallization in a diffusion limited process.[4] Crystallization processes are classically described by Eq. (1), where $\dot{N}$ is the nucleation rate, ΔG^* is the energy barrier to form a critical nucleus, and ΔE_d is the diffusion energy barrier describing the movement of atoms from a matrix into the nucleus

$$\dot{N} = N \exp\left(\frac{\Delta G^*}{kT}\right) \exp\left(-\frac{\Delta E_d}{kT}\right). \quad (1)$$

Both energies can depend on pressure and Eq. (2) describes the effect of pressure on the activation volume for diffusion where D is the diffusivity, p is the pressure, f is the correlation factor, g is a geometrical factor, a is the lattice parameter, and ν_0 is the attempt frequency.[9] For crystalline materials, this model is useful for defect mediated diffusion processes, whereas diffusion associated with interstitial sites is largely independent of pressure

$$V_{act} = -kT\left[\frac{\partial \ln D}{\partial p}\right]_T + kT\left[\frac{\partial \ln(fga^2\nu_0)}{\partial p}\right]_T. \quad (2)$$

Amorphous materials lack long-range order and the onset of crystallization processes depend on pressure.[10] Primary crystallization requires short range diffusion for grain growth. In nanocomposite compositions, growing grains expel Zr and B to the matrix, developing a diffusion barrier that limits grain size. This is useful to reduce magnetocrystalline anisotropy by limiting grain size below the exchange length.[11] Continued heating results in a secondary crystallization process that produces various phases from the amorphous matrix.[12,13] Soft magnetic performance degrades significantly following secondary crystallization and accurate prediction of this phenomenon is important for aging studies of nanocomposites.

Amorphous ribbons of $Fe_{89}Zr_7B_4$ were produced by melt spinning and subsequently hammer milled to approximately 100 μm with thicknesses of 30 μm. Three custom gasket assemblies described by Yamada *et al.* were prepared and loaded in a Paris Edinburgh cell to pressurize and heat on Sector 16-BM-B (HPCAT) at the Advanced Photon Source.[14,15] The pressure medium was a hexagonal boron nitride crucible, which also held a Au pressure marker located in a position perpendicular to the beam direction. Energy dispersive diffraction patterns were collected every 30–60 s at $2\theta = 8°$. These patterns were boxcar averaged to ±3 min to improve counting statistics. Bragg's law can be written conveniently for energy dispersive diffraction where

a)Electronic mail: mm7g@andrew.cmu.edu

the energy for a reflection E_{hkl} is measured in keV and lattice spacing d_{hkl} is given in Å for a fixed angle θ_0[17,18]

$$E_{hkl} = \frac{6.199}{d_{hkl} \sin \theta_0}. \quad (3)$$

The sample table was repositioned periodically to obtain calibration patterns from the Au sample and quickly returned to the sample position. The pressure and temperature of the sample were determined from the equation of state from the Au (022) peak.[16] 2θ Calibration patterns were obtained at room temperature and 1 atm. After pressurizing the anvil, the calculated pressure was assumed to be constant for each respective experiment. This is reasonable since only the small sample volume is heated and the tungsten carbide anvils remain at relatively low temperatures. The cell was heated resistively to temperatures up to 850 °C by a graphite sleeve surrounding the sample to observe the $\alpha \rightarrow \gamma$ Fe transition.

The 2θ value was chosen to optimize resolution and separate Au diffraction peaks from BN crucible and Au fluorescence peaks. Collimation of the incident and scattered beam prevented large signals from the BN or surrounding material. Voigt fits to Au fluorescence peaks were more than 99% Gaussian. Instrument broadening was determined by measuring peak widths for Au diffraction peaks at various 2θ values. Temperature resolution of 1 °C requires a lattice parameter measurement accuracy on the order of 10^{-5} Å. The standard deviation of 50 separate Au fluorescence peak energies was 6 eV, suggesting a temperature error on the order of ±5 °C. Power applied to the cell was adjusted to maintain heating rates between 1.3 and 1.7 °C/min. The calculated pressures for the three runs were 0.5, 2.2, and 4.9 GPa. The degree of deviatoric stress is unknown, but such a state is suggested by smaller d-spacings measured from Au (200) peaks that are sensitive to anisotropic stress.[19]

Figure 1 shows diffraction peaks for the sample upon heating at 2.2 GPa. Each sample showed the same phases present, but their onset temperature and growth rates differed. The as cast sample is amorphous in Fig. 1 and following primary crystallization, the α-Fe phase is present. The BCC phase remains through secondary crystallization, at which point the residual matrix between the grains crystallizes. The Fe grains undergo an $\alpha \rightarrow \gamma$ transformation near 750 °C. Figure 2 shows the areas under the shaded peaks in Fig. 1 (α-Fe (002), a secondary peak centered on 39 keV, and γ-Fe (022)) during heating. The peak areas are normalized to the BCC peak maximum and the sample heated at 4.9 GPa contains a small amount of BCC at room temperature. The onset of primary crystallization for each experiment occurred at 470 ± 10 °C. This value agrees with crystallization studies of NANOPERM at 1 atm.[4,20] The reduced growth rate of primary crystallization and the delay in onset of secondary crystallization in the 4.9 GPa sample is attributed to reduced diffusion at high pressures.

Increased pressure delays secondary crystallization with onset temperatures occurring at 648, 706, and 713 °C for 0.5, 2.2, and 4.9 GPa, respectively. The temperature difference between the onsets of primary and secondary crystallization has also been influenced by glass former content.[21] Reduced glass former content was found to lower secondary crystallization temperature and increase grain size. Grain size measurements are a focus of future efforts. Multiple phases appear at the onset of secondary crystallization including $Fe_{23}Zr_6$, $Fe_{23}B_6$, Fe_3B, and possibly Fe_2B. Evidence of these phases has been found previously in FeCo based nanocomposites.[12,13] Due to the instrument broadening, the amount of secondary crystallization was estimated by integrating a peak centered at 39 keV, which corresponds to the $Fe_{23}B_6$ (115) peak. In the 0.5 GPa experiment, this peak area decreases at 710 °C due to a shift in the neighboring peaks. This is attributed to a reduction in the amount of Fe_3B as shown in Fig. 3. A similar event occurs at 810 °C in the 2.2 GPa sample. This phase transition in the matrix can be attributed to the long range ordering required to form the 23:6 phase and it is believed that the 4.9 GPa sample has not reached temperatures high enough to observe this phase transition.

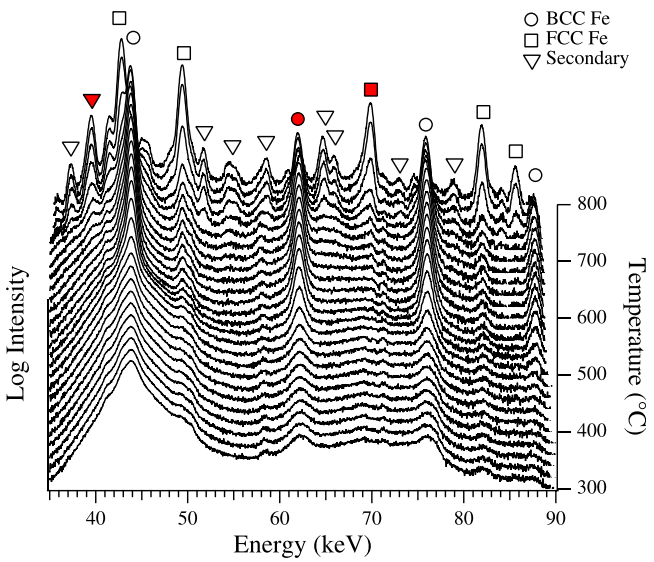

FIG. 1. Labeled diffraction peaks for NANOPERM sample upon heating at 2.2 GPa.

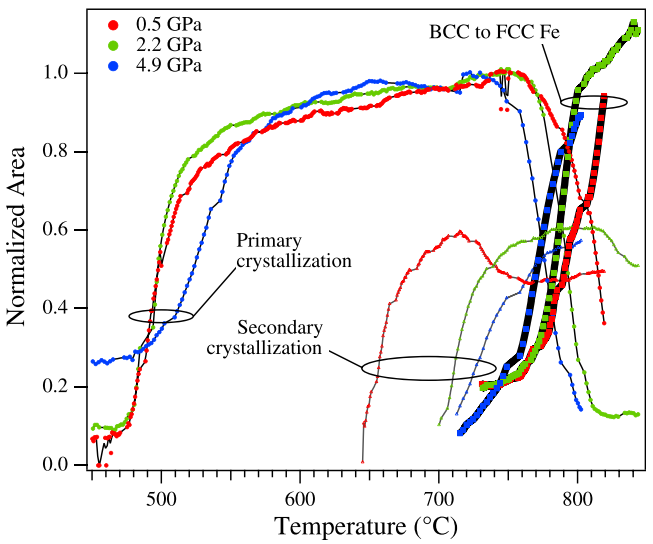

FIG. 2. Peak areas indicating the onset of primary and secondary crystallization and the Fe BCC to FCC transition.

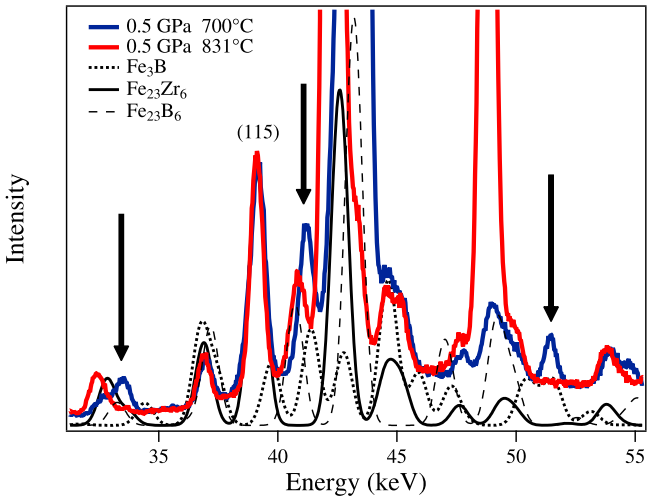

FIG. 3. Secondary crystallization peaks during heating at 0.5 GPa. Arrows indicate changes that can be attributed to the possible conversion of Fe_3B to another phase.

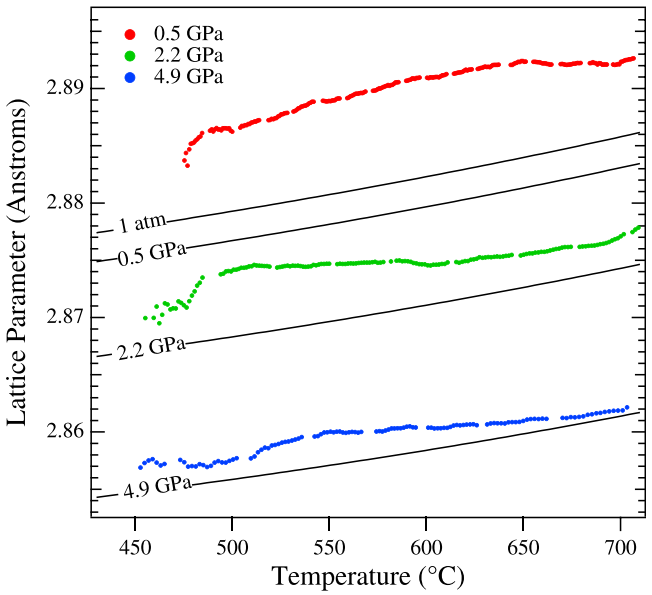

FIG. 4. Comparison of measured nanocrystalline lattice constants to fit to a Vinet equation of state[23] for α-Fe.

The Fe $\alpha \rightarrow \gamma$ transition temperature also lowered from 758 °C at 0.5 and 2.2 GPa to 714 °C at 4.9 GPa in agreement with the pressure experiments on bulk Fe. This is attributed to the lower molar volume of the FCC phase compared to BCC.[22] In Figure 4, the calculated α-Fe lattice parameters for each pressure are compared to a thermal equations of state presented by Sha and Cohen.[23] The expanded lattice parameters can arise from the presence of B and Zr in the crystal matrix and contact with lower density crystal/matrix interface. At higher pressure, the nanocrystalline lattice parameter approaches the value for bulk α-Fe.

The effect of pressures up to 5 GPa on the crystallization of NANOPERM is shown to retard the growth rate during primary crystallization, delay the onset of secondary crystallization, and reduce the $\alpha \rightarrow \gamma$ transition temperature. The effects concerning secondary crystallization are attributed to the long range diffusion required to form the 23:6 phase. The delay of secondary crystallization and the possibility to reduce grain size warrants further study of pressure as a processing tool.

A. M. Leary and M. E. McHenry were supported by ARPA-E Award No. DE-AR0000219 and the ARL through Grant No. W911NF-08-2-0024. Portions of this work were performed at HPCAT (Sector 16), Advanced Photon Source (APS), Argonne National Laboratory. Use of the HPCAT facility was supported by DOE-BES, DOE-NNSA (CDAC), NSF, DOD TACOM, and the W.M. Keck Foundation. Use of the APS was supported by DOE-BES.

[1]M. E. McHenry, M. A. Willard, and D. E. Laughlin, Prog. Mater. Sci. **44**, 291–433 (1999).
[2]A. M. Leary, P. R. Ohodnicki, and M. E. McHenry, JOM **64**, 772–781 (2012).
[3]S. Shen, P. Ohodnicki, S. Kernion, A. Leary, V. Keylin, J. Huth, and M. E. Mchenry, *Nanocomposite Alloy Design for High Frequency Power Conversion Applications* (TMS, 2012).
[4]A. Hsiao, M. McHenry, D. Laughlin, M. Kramer, C. Ashe, and T. Ohkubo, IEEE Trans. Magn. **38**, 3039–3044 (2002).
[5]F. Johnson, C. Um, M. McHenry, and H. Garmestani, J. Magn. Magn. Mater. **297**, 93–98 (2006).
[6]P. R. Ohodnicki, J. Long, D. E. Laughlin, M. E. McHenry, V. Keylin, and J. Huth, J. Appl. Phys. **104**, 113909 (2008).
[7]S. J. Kernion, P. R. Ohodnicki, J. Grossmann, A. Leary, S. Shen, V. Keylin, J. F. Huth, J. Horwath, M. S. Lucas, and M. E. McHenry, Appl. Phys. Lett. **101**, 102408 (2012).
[8]K. Suzuki, A. Makino, A. Inoue, and T. Masumoto, J. Appl. Phys. **74**, 3316 (1993).
[9]F. Faupel, W. Frank, M.-P. Macht, V. Naundorf, K. Ratzke, H. Schober, S. Sharma, and H. Teichler, Rev. Mod. Phys. **75**, 237–280 (2003).
[10]Y. X. Zhuang, J. Z. Jiang, T. J. Zhou, H. Rasmussen, and L. Gerward, Appl. Phys. Lett. **77**, 4133–4135 (2000).
[11]G. Herzer, IEEE Trans. Magn. **26**, 1397–1402 (1990).
[12]J. Long, P. R. Ohodnicki, D. E. Laughlin, M. E. McHenry, T. Ohkubo, and K. Hono, J. Appl. Phys. **101**, 09N114 (2007).
[13]P. Ohodnicki, N. C. Cates, D. Laughlin, M. McHenry, and M. Widom, Phys. Rev. B **78**, 144414 (2008).
[14]A. Yamada, Y. B. Wang, T. Inoue, W. G. Yang, C. Park, T. Yu, and G. Y. Shen, Rev. Sci. Instrum. **82**, 015103 (2011).
[15]G. Shen, P. Chow, Y. Xiao, S. Sinogeikin, Y. Meng, W. Yang, H.-P. Lieermann, O. Shebanova, E. Rod, A. Bommannavar, and H.-K. Mao, High Press. Res. **28**, 145–162 (2008).
[16]O. L. Anderson, D. G. Isaak, and S. Yamamoto, J. Appl. Phys. **65**, 1534 (1989).
[17]B. Buras, D. L. Gerward, J. Jorgensen, and B. Willis, "2.5. Energy-dispersive techniques," in *International Tables for Crystallography, Section 2.5.1* (2006), Vol. C, pp. 84–87.
[18]S. Clark, Crystallogr. Rev. **8**, 57–92 (2002).
[19]T. Duffy, G. Shen, D. Heinz, J. Shu, Y. Ma, H.-K. Mao, R. Hemley, and A. Singh, Phys. Rev. B **60**, 15063–15073 (1999).
[20]S. Stankov, B. Sepiol, T. Kanuch, D. Scherjau, R. Würschum, and M. Miglierini, J. Phys.: Condens. Matter **17**, 3183–3196 (2005).
[21]R. K. Roy, S. J. Kernion, S. Shen, and M. E. McHenry, Appl. Phys. Lett. **99**, 192506 (2011).
[22]M. E. McHenry and M. DeGraef, *Structure of Materials* (Cambridge, New York, 2007).
[23]X. Sha and R. E. Cohen, Phys. Rev. B **73**, 104303 (2006).